ORIGINAL ARTICLE

Groundwater quality assessment in two shallow aquifers with different hydrogeological characteristics (case study: Lenjanat and Babol–Amol aquifers in Iran)

Seyedeh Mona Tabandeh[1] · Majid Kholghi[2] · Seyed Abbas Hosseini[1]

Abstract

Groundwater quality management is based on understanding the spatial distribution of parameters in when assessing the suitability of groundwater for use. In this study, different interpolation methods were evaluated in two shallow aquifers according to their hydrogeological characteristics. After initial data processing, 24 deterministic and geostatistical interpolation methods were used with linear and nonlinear relationships. These included: the inverse distance weighted method; the ordinary kriging; the lognormal ordinary kriging (Log_OK); the universal kriging; the disjunctive kriging; the empirical Bayesian kriging; the simple kriging; natural neighbor; the trend surface; and the Spline methods were compared. The spatial distribution of the total dissolved solids parameter was assessed in the Lenjanat and Babol–Amol shallow aquifers with different hydrogeological characteristics. The seven error criteria were used for verification in cross-validation of all sampling wells. The nonlinear Log_OK method produced better results in the Lenjanat and Babol–Amol aquifers with 57 and 71% of error criteria, respectively. Consequently, the non-linear Log_OK method had promising performance in both shallow aquifers with different hydrogeological characteristics.

Keywords Groundwater contamination · TDS parameter · Shallow aquifer · Linear–nonlinear spatial interpolation · Aquifer characteristics

Introduction

One of the most vital management tools in water resources field is the ability to determine and track the spatial and temporal variations trends of groundwater quality parameters with a high level of confidence. To do this, it is essential that the spatial and temporal distribution of physical and chemical aquifer characteristics are well understood in an aquifer for contamination risk assessment, an issue which does not seem possible without consideration of the spatial relationships of data points (Lee et al. 2007). To this end, geostatistical techniques can be used for this purpose which take the spatial relationships of the distances of the points and also the orientation and values of the variables into consideration. These techniques offer advantages such: an increase in the measurement accuracy of key parameters; and an ability to reduce the sampling density and frequency, which can decrease the cost of sampling programs (Bryan 1988). The geostatistical approach has provided useful techniques for investigating the spatial distribution of data such as groundwater contamination (Arslan 2012; Nas and Berktay 2010). By identifying spatial patterns and undertaking interpolation in locations that lack sufficient information, interpolation analysis can estimate the input parameters of random points in network grid cells using the observed data and, therefore, play an important role in sustainable groundwater management (Arslan 2012; Shan et al. 2013). A paucity of groundwater data results in significant uncertainty (Liu et al. 2004). Geostatistical techniques have been used in various scientific studies in fields such as groundwater assessment, geochemistry, water resources assessment and soil science as a powerful technique to determine the level of uncertainty that is associated with data collection and assessment (Pyrcz and Deutsch 2014; Chilès and Delfiner 2012; Arslan 2012).

✉ Majid Kholghi
  kholghi@ut.ac.ir

[1] Department of Civil Engineering, Science and Research Branch, Islamic Azad University, Tehran, Iran

[2] Department of Irrigation and Reclamation Engineering, University of Tehran, Karaj, Iran

The interpolation methods in geographic information system (GIS) are powerful tools for data interpolation and the prediction of values (Gong et al. 2014). Linear geostatistical methods such as conventional kriging methods are not appropriate due to the smoothing effect which resulted from equation exponents and they also require the calculation of a variogram. Their use, therefore, is often not practical (Chilès and Delfiner 2012; Costa 2003). Nonlinear geostatistical methods, which do not contain the weaknesses of requiring equation exponents and smoothing effects are recommended for the estimation of renewable resources and mapping their spatial characteristics (Emery 2008; Mare'chal 1984).

For example, Martinez-Cob (1996) utilized the three geostatistical interpolation methods of ordinary kriging (OK), co-kriging (Co-K) and modified residual kriging (MRK) for the interpolation of the long-term average of annual reference evapotranspiration and precipitation and found that none of these methods outperform others. Khattak et al. (2014) utilized ordinary and Bayesian kriging (BK) methods to determine the salinity levels of shallow wells in Pakistan and concluded that the second method shows more accuracy. Yao et al. (2014) studied eight interpolation methods to identify the spatial distribution of groundwater levels and showed that the kriging method yielded the best results. Afzal et al. (2015) used ordinary multi-Gaussian kriging (OMK) and simple multi-Gaussian kriging (SMK) for modeling the spatial distribution of iron based on subsurface data in the iron ore deposit. The results indicated that the SMK method was more accurate in moderately and weakly iron mineralized zones, and that the OMK method was more accurate in enriched, highly iron mineralized zones.

Arslan and Turan (2015) compared the interpolation methods of inverse distance weighting (IDW), radial basis function (RBF) and OK to estimate the spatial distribution of 17 heavy metals of groundwater. They found that all of these methods were suitable for estimating the distribution of one or several specific metals. Mirzaei and Sakizadeh (2015) reported the use of IDW, OK, and empirical Bayesian kriging (EBK) interpolation methods in the estimation of 17 groundwater contaminant variables. The results of this investigation indicated that EBK possessed a slightly higher accuracy compared with the two other methods. Plouffe et al. (2015) used IDW, thin plate spline (TPS), OK, and BK methods for the measurement of monthly rainfall in the low and heavy rain months for a 2-year period for minimum and maximum annual rainfall values. They found that BK and TPS methods showed a higher accuracy in the estimation of minimum and maximum rainfall values, respectively. Babu (2016) employed the trend surface (TS), IDW, OK, universal kriging (UK), and Spline methods to assess the spatial and temporal patterns of rainfall. The results of this investigation showed that the TS method demonstrated more accuracy due to the minimum error between the observed and estimated rainfall. However, the OK and UK methods were identified as being the best methods, despite the higher root mean square error (RMSE) values, since they produced a smooth and more realistic interpolated surface. Gol et al. (2017) compared the block kriging, Co-K, and IDW methods with the power of 1, 2, and 4 to estimate the spatial distribution of soil carbon and demonstrated that the Co-K method yielded better results. To estimate electromagnetic levels, Rufo et al. (2018) utilized the spline, IDW, and OK methods after optimizing the characteristic parameters of each method. They reported a higher accuracy using the IDW method. Njeban (2018) investigated the use of the RBF, simple kriging (SK), UK, OK, and IDW methods to measure the spatial distribution of groundwater levels and to produce groundwater level and prediction standard error maps, and found that the UK methods was the method that produced the best results.

However, to date, no study has provided a precise evaluation of how interpolation methods are affected by the characteristics of aquifers that are under investigation. Consequently, this study was undertaken to compare linear and nonlinear interpolation methods to provide a cohesive instruction and guideline for the achievement of the most accurate method based on aquifer type and its characteristics. In this study, the total dissolved solids (TDS) parameter, which is the most widely used parameters for assessing groundwater quality, was measured in two shallow aquifers with different hydrogeological characteristics which are located in two important geographical regions in Iran. The aquifers that were assessed using interpolation techniques were the shallow aquifer that underlies the Lenjanat plain of Isfahan, and the shallow aquifer beneath the Babol–Amol plain of Mazandaran area. The study was undertaken using a combination of 24 different interpolation methods including the inverse distance weighted (IDW), OK, lognormal ordinary kriging (Log_OK), universal kriging (UK), disjunctive kriging (DK), EBK, simple kriging (SK), natural neighbor (NN), trend surface (TS) and Spline interpolation methods with seven error parameters in cross-validation of all sampling wells. In the end, the best interpolation method was introduced based on the aquifer characteristics.

Methodology and materials

Study area

In this research, two shallow aquifers have been studied: one is located in the center of Iran and another one located in the north of Iran near the Caspian Sea shore. A location map of the study areas is illustrated in Fig. 1.
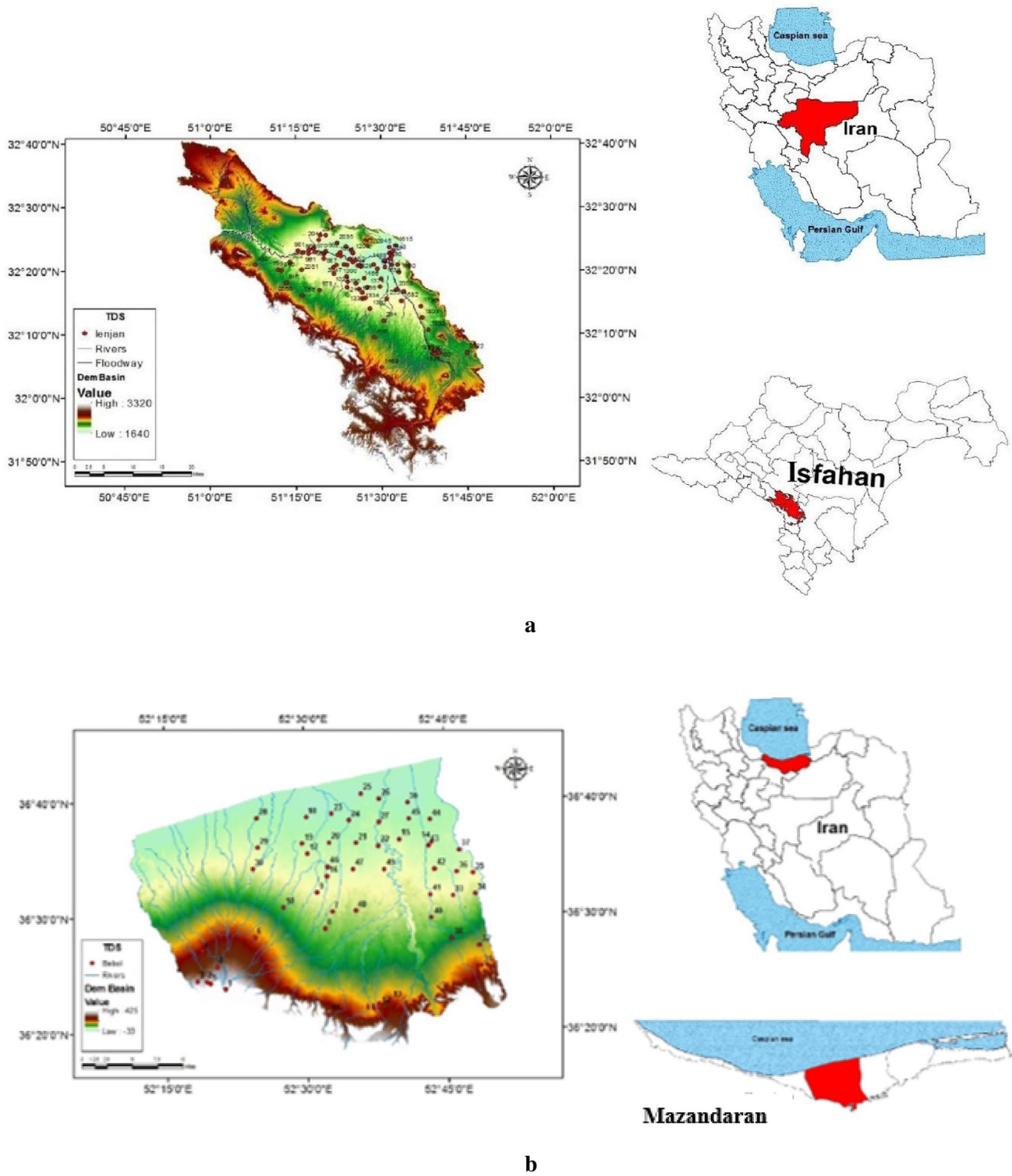
a

b

Fig. 1 Location of the study area with spatial distribution of sampling wells: a Lenjanat **b** Babol–Amol

Lenjanat aquifer

Area description This aquifer, has an area of 1189 km^2 and is located between longitudes 51° 2′ to 51° 47′ and latitudes 31° 53′ to 32° 31′, in the southwestern part of Isfahan province in the center of Iran. The average annual precipitation and temperatures in the area are equal to 209 mm and 12.46 °C, respectively.

One of the most important rivers in Iran, the Zayandehrud River, in an easterly direction through the plain and has an average discharge rate of 42 m³/s. Furthermore, the Salt River is located in the southern half of the region with an average discharge of 12.2 million cubic meters (MCM) per year that is used for agriculture.

Based on groundwater potentiometric head contours and the topography of the area, the groundwater discharges into the Zayandehrud River in a 26 km reach from the entrance to the Lenjanat aquifer. On the other hand, this river recharges the aquifer in the remaining 17 km due to the high rate of groundwater withdrawal in the area.

Two of the most important industrial facilities in the country are located in this area. These are Isfahan and Mobarekeh Steel Co. which has 28,000 employers). The main and traditional activity of the population is agriculture and consequently 400,000 ha of the study area is used for the irrigated cultivation of wheat, barley and rice.

The water demand of the plain is supplied by groundwater abstraction from the underlying aquifer, from rivers, from karst springs, and from Qanats (sloping underground channels in an aquifer).

The Lenjanat aquifer is the most significant water source as groundwater pumped from this aquifer supplies 70% of the water demand for the industrial, agricultural and domestic sectors in the study area. A map of the study area is illustrated in Fig. 1a.

Hydrogeological characteristics The Lenjanat aquifer consists of alluvial sediments and is unconfined. The main source of its recharge is precipitation. The bedrock of the Lenjanat aquifer is Jurassic shale and, in some areas, Cretaceous limestone. The deepest alluvial layers that are deposited at the top of the bedrock are fine clay-marl sediments,

which have a higher percentage of salt than other sediments. This layer is highly impermeable due to its degree of compaction.

Evaporite minerals have developed in the form of gypsum and salt layers and crystals within these sediments. The percentage of salt and clay in the sediments increases in the lower layers. The thickness of young alluvial sediments gradually increases at the intersection of flood channels towards Zayandehrud. In the middle areas of the plain, the thickness of sediments reaches more than 150 m. Based on geophysical studies, the average saturated thickness of the aquifer is about 50 m.

Despite the anisotropy of alluvial sediments beneath the plain, impermeable horizons are not observed among discontinuous sediments and subsurface information indicates the existence of an unconfined aquifer in the Lenjanat plain. The geological map of this area is shown in Fig. 2a.

The transmissivity of aquifer varies from 600 to 2000 m²/day and average specific yield is 2%. The spatial variation of transmissivity is illustrated in Fig. 3a.

The depth of groundwater level varies from 2 m near the Zayandehrud River to about 50 m in the center of the plain. The hydraulic gradient varies between 3 and 21 m/1000 m. The groundwater level map and streamlines are shown in Fig. 4a.

In this study area, the aquifer output from the pumping wells, spring, and Qanat for industrial, agricultural and domestic water demands are 132, 1.4, and 57 MCM, respectively. A 6 MCM negative groundwater budget was calculated in this aquifer for the study year.

Based on geochemical evidence, the variation of EC depends on partial dissolution of evaporite minerals in the aquifer sediments.
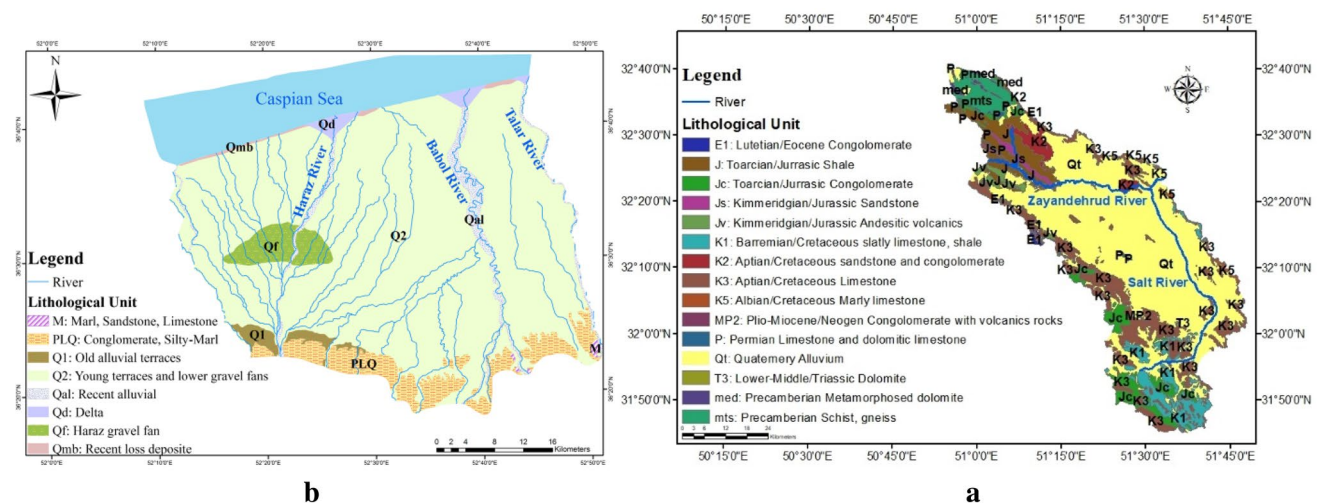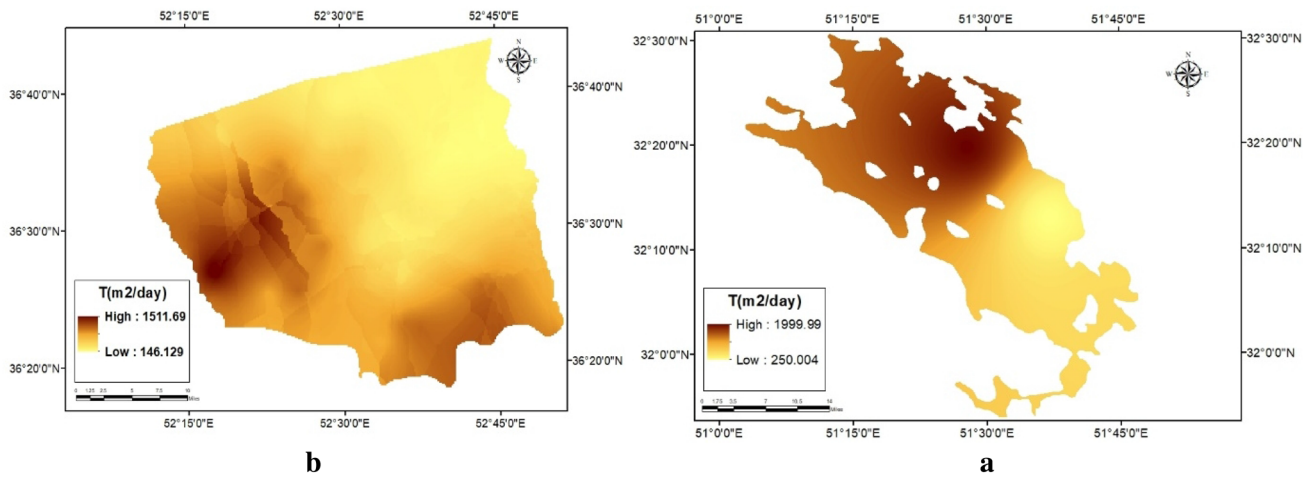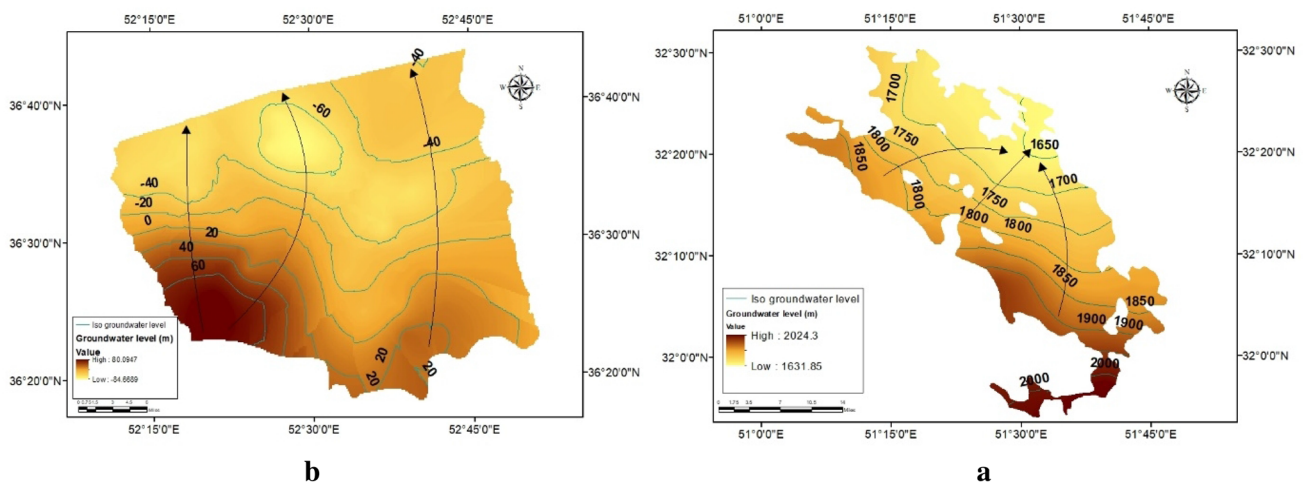

Fig. 2 Geology maps of: **a** Lenjanat aquifer **b** Babol–Amol aquifer

Fig. 3 Transmissivity spatial distribution maps of: **a** Lenjanat aquifer **b** Babol–Amol aquifer

Fig. 4 Groundwater-level maps and streamlines of: **a** Lenjanat aquifer **b** Babol–Amol aquifer

Due to the presence of calcareous formations in sediments that enclose the plain, groundwater in the aquifer is dominantly a calcium bicarbonate composition type.

The dissolution of halite in aquifer sediments leads to the evolution of the anionic composition of groundwater along flowpaths, with a progressive change from bicarbonate dominance to sulfate and then to chloride dominance with the formation of Cl–Na facies groundwater. The release of sodium ions into groundwater due to the dissolution of halite and the contact of groundwater with alluvial marl sediments causes Na absorption and the release of Ca into groundwater and the formation of Cl–Ca facies in the middle of the plain. Recent geochemical changes in this part of the aquifer have caused the groundwater electrical conductivity (EC) to increase by more than 11,000 μmoh/cm.in a few points.

The EC of groundwater in this area varies from 700 to 8500 μmoh/cm. It usually decreases during spring rainfalls.

The total dissolved solids (TDS) data were calculated from EC measurements using the following equation (Rhoades et al. 1999):

$$TDS(ppm) = 0.64 \times EC(\mu moh/cm), \tag{1}$$

The TDS level map (ppm) including main rivers of aquifer is shown in Fig. 5a.

The Babol–Amol aquifer

Area description This aquifer has an area of 1445 km^2 and lies between longitudes 52°11′ to 52° 52′ and latitudes f 36° 18′ to 36° 44′ It is located in a coastal region (Caspian Sea Coast) of the Mazandaran province in the north of Iran. The average annual rainfall and temperatures of the region are 870 mm and 17.9 °C, respectively.
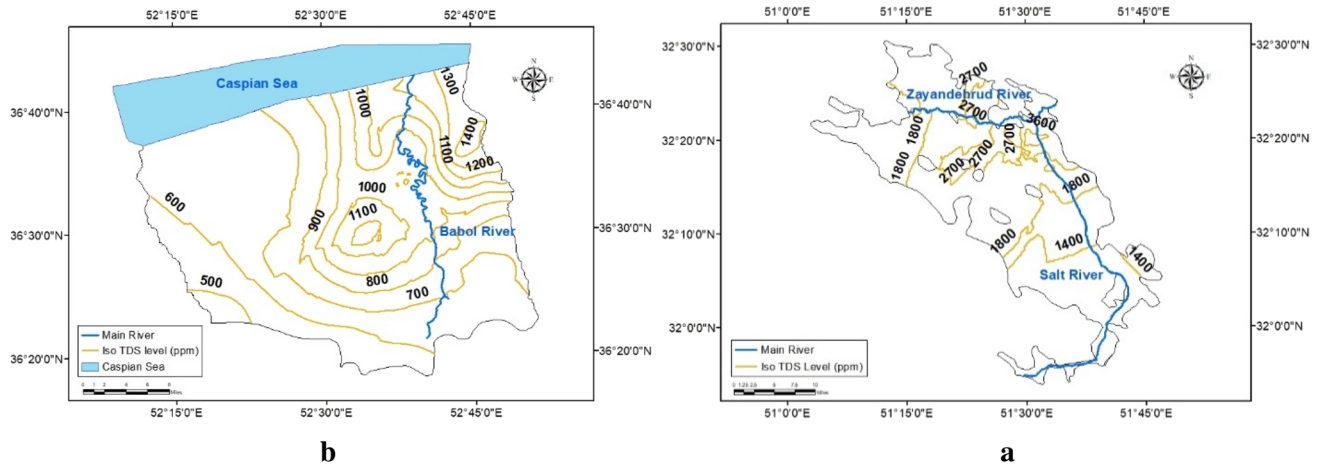
Fig. 5 TDS-level maps with main rivers of: **a** Lenjanat aquifer **b** Babol–Amol aquifer

Three main rivers, the Babol, Haraz, and Talar rivers, flow from the south to the north of the plain with average discharge rates of 493, 940, and 311 MCM/year, respectively. The main sources of these rivers, are snowmelt and precipitation. After the irrigation of a large area of agricultural land, these rivers enter the Caspian Sea. The main and traditional activity of the local people is agriculture and horticulture with a 101,000 ha irrigated area that is cultivated for rice and oranges. Both groundwater and water from the rivers are used as sources of irrigation water. Rivers in the area are both sources of groundwater recharge and receive groundwater discharge.

The Babol–Amol aquifer plays an important role in this area as the supplier of 63% water demand in the agricultural–horticulture and domestic sectors. The general map of the study area is illustrated in Fig. 1b.

Hydrogeological characteristics The Babol–Amol aquifer is alluvial and unconfined. The main source of its recharge is precipitation and leakage through riverbeds. The bedrock of this aquifer is clay.

The alluvial fan deposits are usually coarse-grained and include rubble, sand, which are alternated with fine-grained sediments such as clays and silts. The granulation and material of discontinuous sediments in lateral expansion and depth are very different in this plain. The western regions of the Babol–Amol aquifer are affected by the Haraz River and have created a deep basin with a large thickness of alluvial sediments, which has been extended to the Caspian Sea. The sediment-resistant zones in the central and eastern part of the area have been formed under the influence of Sajadrud alluvial fans and the Babol and Talar Rivers. This basin has a limited expansion compared to the Haraz sedimentary basin. The geological map of the area is shown in Fig. 2b.

According to the results of pumping tests, the transmissivity of the Babol–Amol aquifer varies from 146 to 1512 m^2/day and the average specific yield is 6%. The western part of the plain has a higher transmissivity compared to the eastern part due to the expansion of alluvial of the Haraz River. The spatial variation of the transmissivity of the aquifer in the area is shown in Fig. 3b.

The depth of the groundwater level varies from 0.5 to 37 m and the hydraulic gradient variation in this aquifer is between 2.4 and 5.5 m/1000 m. Based on the geophysical survey results, the average saturated thickness of the Babol–Amol aquifer is about 80 m. The groundwater levels and streamlines are illustrated in Fig. 4b.

In the study area, aquifer output from pumping wells for agricultural and domestic water demands are 323 MCM and a there is a 69 MCM negative average groundwater budget during a period of 12 years with a groundwater level decline of 0.8 m.

In terms of hydrogeochemistry, the EC of groundwater in the Babol–Amol aquifer varies from 500 to 3000 μmoh/cm, which was transformed into TDS. The TDS level map (ppm) including main rivers of the aquifer is shown in Fig. 5b.

Data sources

The sampling wells are homogenously distributed in the region so that they represent the characteristics of the whole aquifer. The quality sampling well network is suitable and covers the all of aquifer zones. The sampling wells in saturated layer of aquifer are all screened.

The TDS samples which are collected from 72 observation wells of Lenjanat aquifer and 50 observation wells of the Babol–Amol aquifer were obtained from the Isfahan Regional Water Organization, Isfahan Water and Wastewater company, and the Department of Environment of Tehran for

a period of 14 water years between 1995 and 2009, respectively. The locations of the observation wells, which were uniformly distributed across the aquifer to indicate the whole area hydrogeological characteristics, are illustrated in Fig. 1.

The statistical and mathematical basics

This study made use of primary concepts of geostatistics such as the definitions of isotropy and anisotropy and different interpolation methods which were used in many studies. For more information refer to Mastroianni and Milovanovic (2008) and Duffy and Germani (2013). As depicted in Table 1, the methods used in this study including IDW, OK, Log_OK, UK, DK, EBK, SK, NN, TS, and Spline were identified as the superior methods in prior studies. This section only provides an explanation of the Log_OK method which is the most accurate interpolation method of this study.

Lognormal ordinary kriging (Log_OK)

Despite the nonlinear interpolation methods, skewed data cannot be used in linear interpolation, because there would be incompatibility of variance with the average. The solution of this problem is a proper approach based on transformation data (Roth 1998). It is better to use one of the linear interpolation methods such as OK to estimate the data after normalization using the appropriate transformation method. In next step, the estimated values are transformed into real values using the back-transformation approach (Isaaks and Srivastava 1989).

If $Z(x)$ represents the value of regional variable at a point with the location of x at unobserved points in a region D, so that the normal distribution of $Z(x)$ is $Y(x) = \ln Z(x), x \in D$, the objective is to estimate the value of the regional variable of $Z(x)$ (Yamamoto 2000). The main step is the transformation of the problem from Z to stationary normal distribution, Y. The value of $Y(x_0)$ is estimated as follows:

$$\widehat{Y}(x_0) = \sum_{i=1}^{n} \lambda_i \ln Z(x_i) = \sum_{i=1}^{n} \lambda_i Y(x_i), \tag{2}$$

where $\widehat{Y}(x_0)$ is the estimated value of $Y(x_0)$, λ_i is the weight of kriging, and n is the total observed data.

Back-transformation of $\widehat{Y}(x_0)$ to $\widehat{Z}(x_0)$ is skewed based on the following equation:

$$\widehat{Z}(x_0) = \exp\left(\widehat{Y}(x_0) + \frac{\sigma_{Y,K}^2}{2} - m_Y\right), \tag{3}$$

where $\widehat{Z}(x_0)$ is the estimated value of $Z(x_0)$, $\sigma_{Y,K}^2$ is the kriging variance of Y, and m_Y is the Lagrange multiplier value (Cressie 1993). A detailed explanation of this method

is provided in the reference books of Journel and Huijbregts (1978) and Dowd (1982).

Accuracy analysis of different interpolation methods

Cross validation is one of the most widely used methods to compare the performance of interpolation methods (Yao et al. 2014). In this method, one of the observed points $(Z(x_i))$ from the set of input data $\{Z(x_1), \ldots, Z(x_n)\}$ is eliminated. Then, the value of the variable at location x_i $(Z^*(x_i))$ is estimated using other data with one of the interpolation methods. This process must be repeated until all input data is estimated (Kitanidis 1993).

In this study, the cross-validation of all sampling wells was used to estimate the best interpolation method. Then seven error criteria were calculated using mean error (ME), mean bias error (MBE), mean absolute error (MAE), mean relative error (MRE), mean squared error (MSE), root mean squared error (RMSE), Nash–Sutcliffe efficiency (NSE) and percentage BIAS (PBIAS):

$$\text{ME or MBE} = \frac{1}{n} \sum_{i=1}^{n} \left(Z^*(x_i) - Z(x_i)\right), \tag{4}$$

$$\text{MAE} = \frac{1}{n} \sum_{i=1}^{n} \left|Z^*(x_i) - Z(x_i)\right|, \tag{5}$$

$$\text{MRE} = \frac{1}{n} \sum_{i=1}^{n} \left|\frac{Z^*(x_i) - Z(x_i)}{Z(x_i)}\right|, \tag{6}$$

$$\text{MSE} = \frac{1}{n} \sum_{i=1}^{n} \left[Z^*(x_i) - Z(x_i)\right]^2, \tag{7}$$

$$\text{RMSE} = \left[\frac{1}{n} \sum_{i=1}^{n} \left[Z^*(x_i) - Z(x_i)\right]^2\right]^{1/2}, \tag{8}$$

$$\text{NSE} = 1 - \frac{\sum_{i=1}^{n} \left[Z(x_i) - Z^*(x_i)\right]^2}{\sum_{i=1}^{n} \left[Z(x_i) - O\right]^2}, \tag{9}$$

$$\text{PBIAS} = \frac{\sum_{i=1}^{n} \left[Z(x_i) - Z^*(x_i)\right]}{\sum_{i=1}^{n} Z(x_i)} * 100, \tag{10}$$

where $Z^*(x_i)$ is the interpolated value for ith well, $Z(x_i)$ is the observed value for ith well, n is the number of all wells, and O is the average value for all the observation wells (Xie et al. 2011).

Due to the dependence of these values to data scale, the use of standardized error is recommended (Krivoruchko 2011). The best fit model is the one in which the standard

Table 1 Superior methods of the previous studies

Case study	Field	References	Compared methods	Best method
1	Agriculture and soil science	Van Kuilenburg et al. (1982)	NeN, IDS, OK	OK
2	Geoscience	Puente and Bras (1986)	UK, DK, local mean estimator	UK
3	Agriculture and soil science	Laslett et al. (1987)	TPS, OK, global means and medians, NeN, IDW, IDS, AK, NN, Trend	OK and TPS
4	Computer and geoscience	Isaaks and Srivastava (1989)	OK, IDS, TIN, NeN	OK
5	Geoscience	Boufassa and Armstrong (1989)	OK, Log_OK, SK, lognormal SK, disjunctive OK, disjunctive SK	OK and SK
6	Meteorology and water resources	Hosseini et al. (1993)	OK, UK, IDW, AK, trend	OK
7	Agriculture and soil science	Gotway et al. (1996)	OK, IDW	OK
8	Agriculture and soil science	Kravchenko and Bullock (1999)	OK, Log_OK, IDW	Log_OK
9	Agriculture and soil science	Hartkamp et al. (1999)	IDW, TPS, OCK	Similar
10	Geoscience	Zimmerman et al. (1999)	OK, UK, IDS	OK
11	Agriculture and soil science	Schloeder et al. (2001)	OK, IDW, TPS	OK and IDW
12	Agriculture and soil science	Moyeed and Papritz (2002)	OK, Log_OK, DK, IK, MBK	Similar
13	Agriculture and soil science	Meul and Van Meirvenne (2003)	OK, UK, SKlm, OCK	UK and OCK
14	Meteorology and water resources	Sterling (2003)	IDW, Spline-r, Spline-t, TPS, MS, IMS, OK, SK, UK	SK and TPS
15	Meteorology and water resources	Vicente-Serrano et al. (2003)	LM, NeN, IDW, splines, trend, SK, OK, BK, UK, OCK, LM with IDS, splines with LM	Kriging and LM
16	Agriculture and soil science	Hu et al. (2004)	SK, OK, Lognormal kriging, UK, DK, IDW	UK
17	Meteorology and water resources	Naoum and Tsanis (2004)	Splines, IDW, NeN, LM, OK, UK	OK and UK
18	Environmental science	Dick and Gerard (2006)	OK, UK, LM	UK
19	Meteorology and water resources	Barca and Passarella (2007)	DK, conditional geostatistical simulation	DK
20	Meteorology and water resources	Hua et al. (2009)	IDW, Ok	OK
21	Meteorology and water resources	Chiu et al. (2009)	OK, DetOK, AniOK, OCK, ResOK, Log_OK	Log_OK
22	Meteorology and water resources	Sun et al. (2009)	IDW, RBF, OK, UK, SK	SK
23	Meteorology and water resources	Keblouti et al. (2012)	IDW, OK, Spline	IDW
24	Environmental science	Joseph et al. (2013)	IDW, NeN, OK, UK, simple average	OK
25	Computational fluid dynamics	Wang et al. (2013)	POD, spline	Spline
26	Mathematics and computer science	Aguilera and Aguilera-Morillo (2013)	P-spline, smoothing spline, regression spline	P-Spline
27	Marine science	Liu et al. (2014)	IDW, LPI, OK, DK	DK
28	Meteorology and water resources	Gong et al. (2014)	IDW, OK-Gaussian, OK-spherical, OCK	IDW
29	Meteorology and water resources	Khattak et al. (2014)	OK, EBK	EBK
30	Meteorology and water resources	Yao et al. (2014)	IDW, GPI, LPI, Spline-r, Spline-t, Ok, UK, SK	OK
31	Meteorology and water resources	Mirzaei and Sakizadeh (2015)	IDW, OK, EBK	EBK
32	Meteorology and water resources	Plouffe et al. (2015)	IDW, TPS, OK, EBK	EBK and TPS
33	Geoscience	Szypuła (2016)	IDW, NN, Spline, RBF, kriging, LPI	Kriging and NN
34	Geoscience	Babu (2016)	IDW, Spline-r, Spline-t, trend, Ok, UK	Ok, UK, Trend
35	Meteorology and water resources	Salekin et al. (2018)	IDW, NN, TR	TR and NN
36	Environmental science	Rufo et al. (2018)	IDW, OK, Spline	IDW
37	Meteorology and water resources	Njeban (2018)	IDW, OK, UK, SK, RBF	UK

error of ME, MSE, and PBIAS is close to zero, NSE is close to 1, and contain the lowest values in RMSE, MAE, MRE.

Study procedure

This study made use of ArcGIS 10.5 software in the following processes:

Data analysis

Spatial autocorrelation of data Data semi-variograms were produced by the GIS software using the OK method. If the semi-variogram of the spatial data increases regularly with the increase in the distance until it reaches the sill, the data will have an appropriate spatial correlation.

Removing local and global outliers Usually, in the presence of global outliers, the semi-variogram is divided into two completely separate parts consisting of upper sparse and dense points. To detect global outliers, first the sparse points at the upper layer of semi-variogram were selected and their locations were marked on the map. Then, one or two specific points, in which all the selected points were joined, were recognized. These specific points were global outliers which were removed due to the lack of logical reasoning and the measurement error (Krivoruchko 2011).

Removal of the local outliers was performed by the clustering and Voronoi section of the GIS software. A Voronoi polygon was made around each of the TDS observation wells. Considering the range of data variability, the polygons were subdivided into several clusters. In the absence of common cluster between each Voronoi cell and neighbor polygons, that cell is potentially an outlier and is shown in grey. After the analysis of the hydrogeological characteristics of observation wells located in the grey Voronoi polygon, in case of the absence of logical reasoning, these points were considered as local outliers and were removed from the network.

Data trend identification The identification of the data trend is important for the selection of an interpolation method. Therefore, the trend analysis of the data in two north–south and east–west directions was performed.

Interpolation and providing spatial distribution maps of groundwater contamination

In addition to the type of interpolation method, the method parameters including the number of effective neighboring points for estimating unknown points, the type of semi-variogram model, the size of the lags of the semi-variogram model, the number of lags, the overlaying factor, the number of simulations, etc. are influential in determining the accuracy of the results. To this end, after processing the data and optimizing the parameters related to each method, TDS interpolation was performed with cross-validation of the different interpolation methods. Subsequently, TDS spatial distribution maps were generated to compare the difference between the contamination estimations in different interpolation methods, and also to select the best method. Eventually, the superior method was selected based on error criteria and was used for generating the TDS spatial distribution maps after determining its compatibility with the hydrogeological characteristics of the aquifer. Based on the standards of the World Health Organization (WHO), the TDS threshold selected was 1200 parts per millions (ppm). The flowchart of the study methodology is provided in Fig. 6.

Results and discussion

The produced maps using 24 different linear and nonlinear interpolation methods are demonstrated in Fig. 7. These methods were used to assess TDS levels in a total of 122 observation wells in two different characteristics shallow aquifers of Lenjanat and Babol–Amol, so that the obtained results would be able to demonstrate the different conditions of the aquifers in general. The produced maps show a high concentration of TDS in the northern, eastern, and central boundaries of the Lenjanat aquifer, which was justifiable regarding the location of the industrial sites, factories, cemeteries and wastewater plants of Zarinshahr and Safaeiyeh which are generally in the east-northern and central parts of the Lenjanat plain. Spatial distribution maps indicated TDS concentrations in the northern, northeastern, and central parts of the Babol–Amol aquifer. The results made sense with the regional geological formations and the land uses in the Qaemshahr city neighborhood in the south of Babol. As predicted, the quality of groundwater decreased with the flow of water into downstream of the aquifer which was mainly the result of the leach-scour of the municipal and agricultural sewage which conformed to the TDS spatial distribution maps of Fig. 7. Besides, the reduction of groundwater quality downstream of the studied areas was congruent with distribution of the population which is greater in downstream areas than elsewhere in the study areas.

Table 2 illustrates the criteria of standard cross validation of the TDS parameter related to different interpolation methods in two shallow aquifers of Lenjanat and Babol–Amol with different hydrogeological
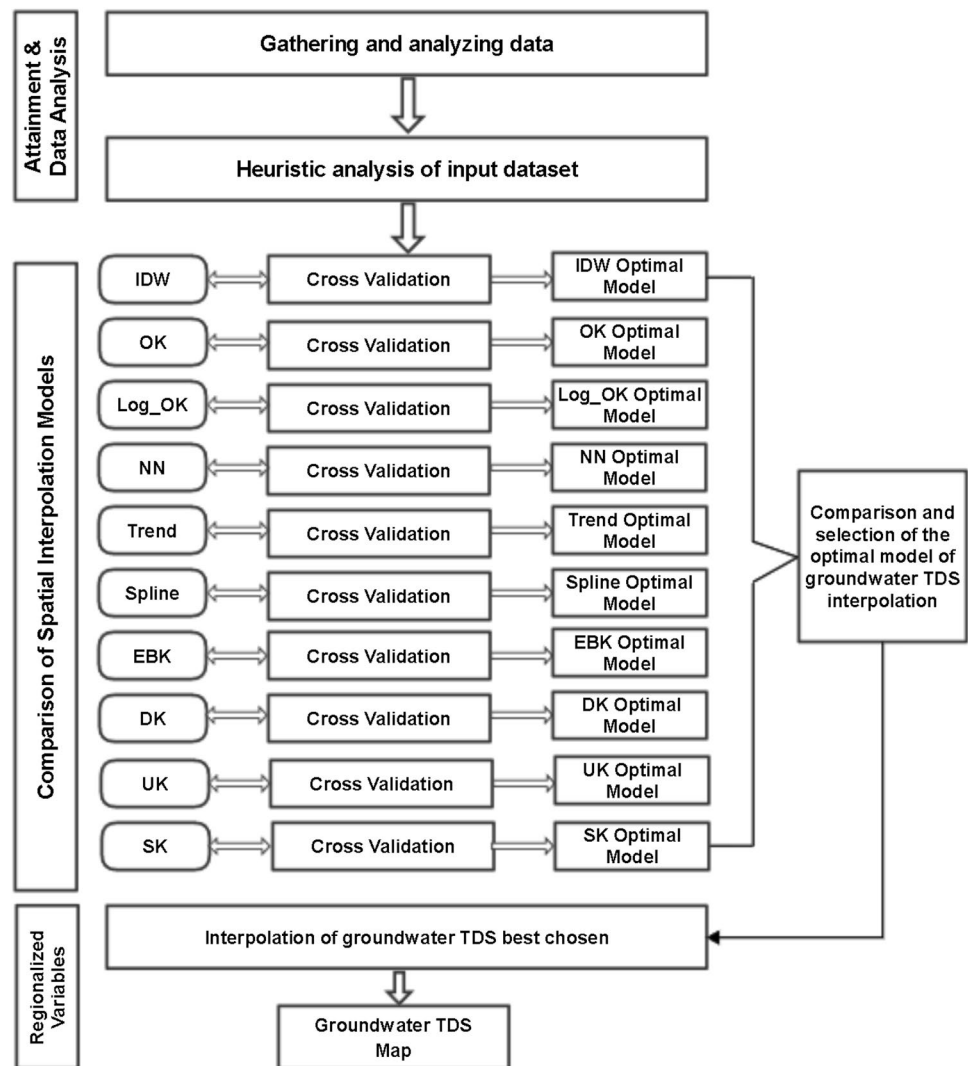
characteristics. In the Lenjanat shallow aquifer, Log_OK had the best results concerning the RMSE value. Next comes the IDW methods with the respective power of 4 and 3 given the lowest RMSE values compared to the other methods. |ME| near to zero demonstrated the less skewedness of the data. Spline-t, SK, and Log_OK with the lowest |ME| values yielded better results, respectively. Log_OK produced the best result with the lowest values of MAE and MSE. Log_OK, NN, and IDW_4, with NSE close to 1, contained the best prediction accuracy, respectively. IDW_4, Log_OK, and IDW_3, with the lowest MRE values, were identified as the best methods, respectively. Spline-t with the lowest |PBIAS| yielded the best results. After that, minimal |PBIAS| was obtained by SK

and Log_OK, respectively. The weight parameter had a significant effect on the accuracy of interpolation so that the more IDW power leads to lower values of RMSE, |ME|, MAE, MRE, MSE and PBIAS and greater NSE.

In the Babol–Amol shallow aquifer, Log_OK produced the best result with the lowest amount of RMSE, MAE, MRE, and MSE. Trend-1 yielded the most accurate result with the lowest values of ME. EBK-emp and EBK-logemp came in the next rank, respectively. Log_OK and EBK-logemp, with NSE closer to 1, demonstrated the best results. The lowest |PBIAS| belonged to Trend-1. With the increase in the IDW power, there was a decrease in the values of MAE and MRE and an increase in NSE.
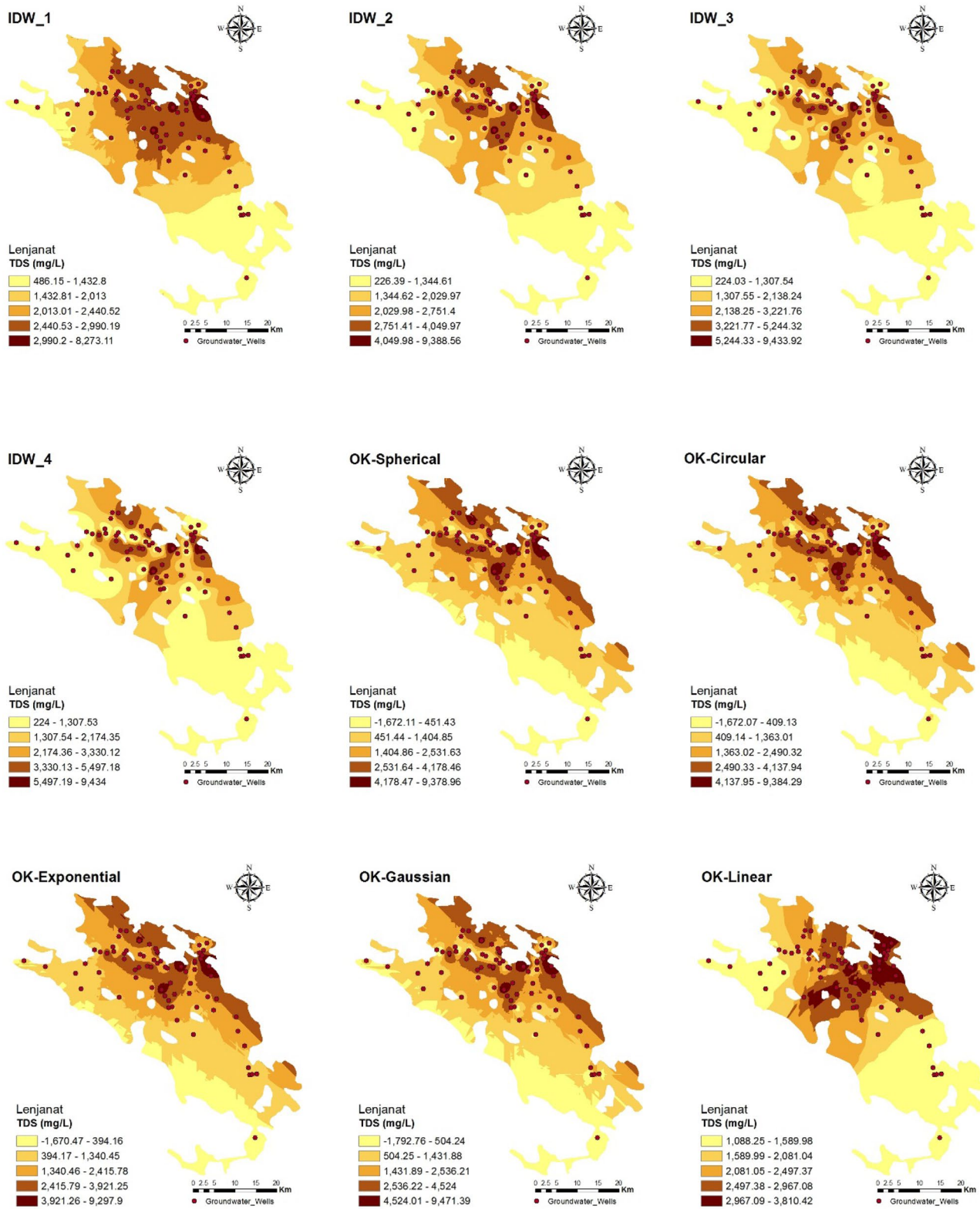
a

Fig. 7 Interpolated maps for TDS using different interpolation methods of: **a** Lenjanat aquifer **b** Babol–Amol aquifer (the legend indicates the predicted TDS concentration)

UK-Linear drift

Lenjanat
TDS (mg/L)
- -2,931.85 - -50.28
- -50.27 - 1,364.32
- 1,364.33 - 2,778.91
- 2,778.92 - 5,031.77
- 5,031.78 - 10,428.17
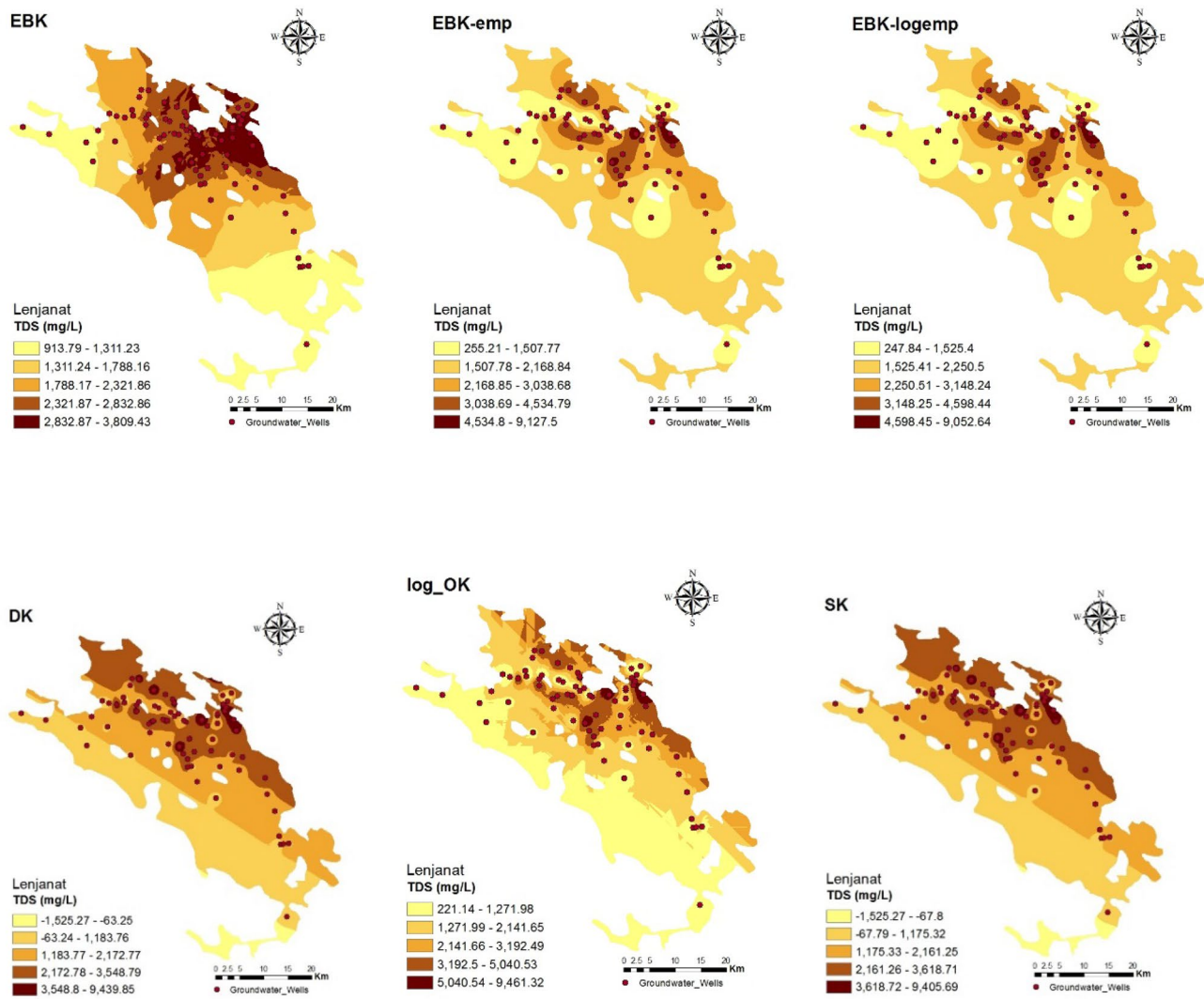- Groundwater_Wells

UK-Quadratic drift

Lenjanat
TDS (mg/L)
- -52,508.3 - -16,675.38
- -16,675.37 - -3,238.04
- -3,238.03 - 2,619.27
- 2,619.28 - 9,165.67
- 9,165.68 - 35,351.27
- Groundwater_Wells

NN

Lenjanat
TDS (mg/L)
- 241.38 - 1,017.79
- 1,017.8 - 1,900.08
- 1,900.09 - 2,994.12
- 2,994.13 - 4,617.53
- 4,617.54 - 9,240.72
- Groundwater_Wells

Spline-r

Lenjanat
TDS (mg/L)
- -26,321.6 - -10,978.33
- -10,978.32 - -2,550.33
- -2,550.32 - 3,716.64
- 3,716.65 - 11,928.53
- 11,928.54 - 28,568.41
- Groundwater_Wells

Spline-t

Lenjanat
TDS (mg/L)
- -1,118.96 - 57.28
- 57.29 - 1,275.53
- 1,275.54 - 2,829.85
- 2,829.86 - 4,888.27
- 4,888.28 - 9,593.23
- Groundwater_Wells

Trend-1

Lenjanat
TDS (mg/L)
- -1,448.36 - -136.23
- -136.22 - 1,011.88
- 1,011.89 - 1,749.96
- 1,749.97 - 2,508.53
- 2,508.54 - 3,779.66
- Groundwater_Wells

Trend-2

Lenjanat
TDS (mg/L)
- -1,732.68 - -225
- -224.99 - 851.92
- 851.93 - 1,595.97
- 1,595.98 - 2,320.44
- 2,320.45 - 3,260.29
- Groundwater_Wells

Trend-3

Lenjanat
TDS (mg/L)
- -1,220.67 - 1,484.97
- 1,484.98 - 4,190.61
- 4,190.62 - 7,326.7
- 7,326.71 - 10,278.31
- 10,278.32 - 14,459.75
- Groundwater_Wells

Trend-4

Lenjanat
TDS (mg/L)
- -3,528.58 - -829.58
- -829.57 - 1,483.85
- 1,483.86 - 4,664.81
- 4,664.82 - 10,159.21
- 10,159.22 - 21,051.6
- Groundwater_Wells

a

Fig. 7 (continued)

Fig. 7 (continued)

As a result, the Log_OK method provided more accurate results with 57% of the error criteria in the Lenjanat shallow aquifer and 71% in the Babol–Amol shallow aquifer. However, the IDW method also had a reliable performance.

Conclusions The present research, for the first time, compared the accuracy of 24 interpolation methods in estimating the spatial variation of groundwater TDS concentration in two shallow aquifers with different hydrogeological characteristics. The main contributions of this study were as follows:

1. In the Lenjanat shallow aquifer, Log_OK produced the best result with the lowest values of MAE and MSE. Log_OK, NN, and IDW_4, with the NSE closer to 1, contained the best prediction accuracy, respectively. IDW_4, Log_OK, and IDW_3, with the lowest MRE values, were identified as the best methods, respectively. Spline-t with the lowest |PBIAS| yielded the best results. After that, minimal |PBIAS| is obtained by SK and Log_OK, respectively.

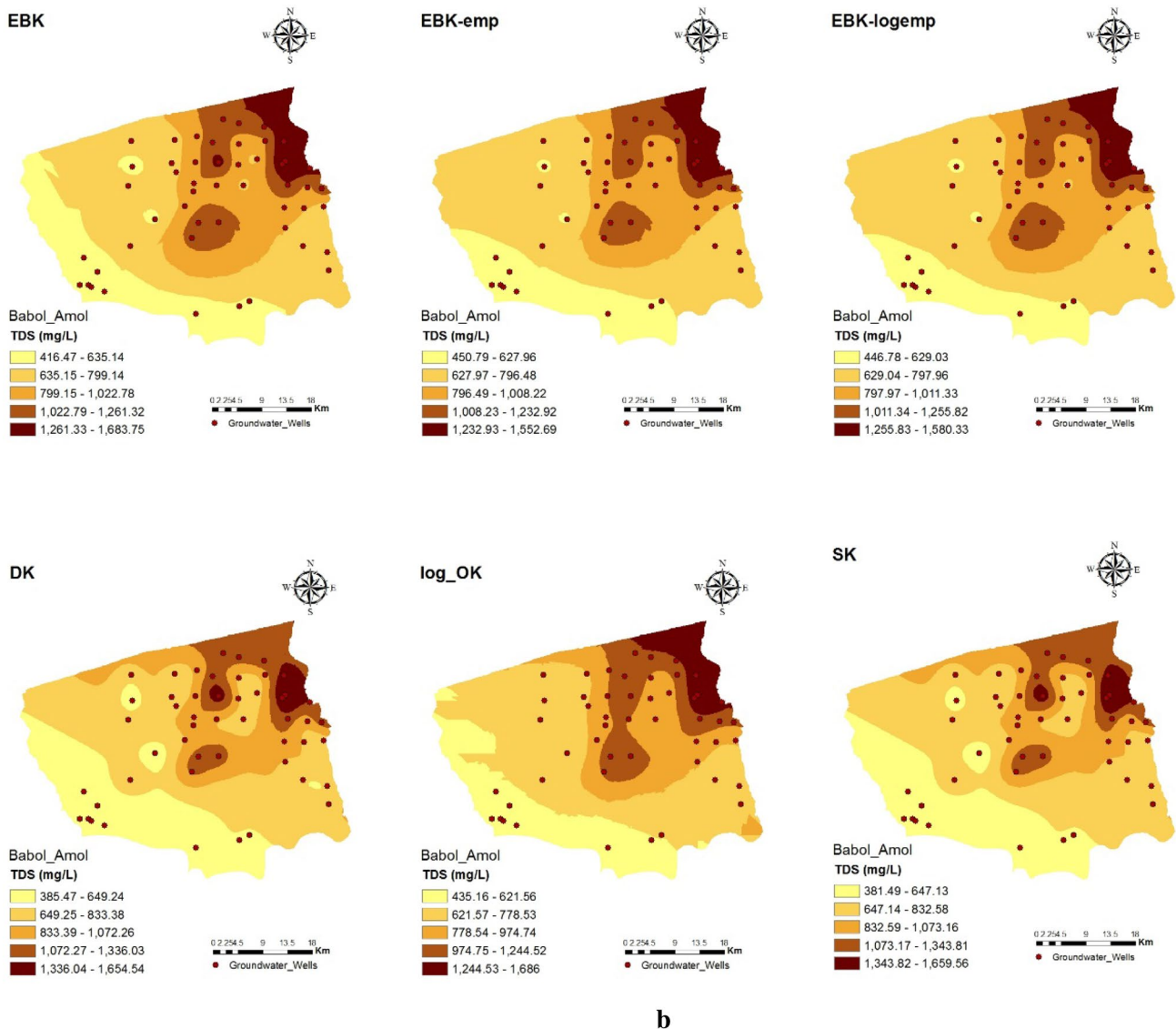2. In the Babol–Amol shallow aquifer, Log_OK produced the best result with the lowest amount of RMSE, MAE,
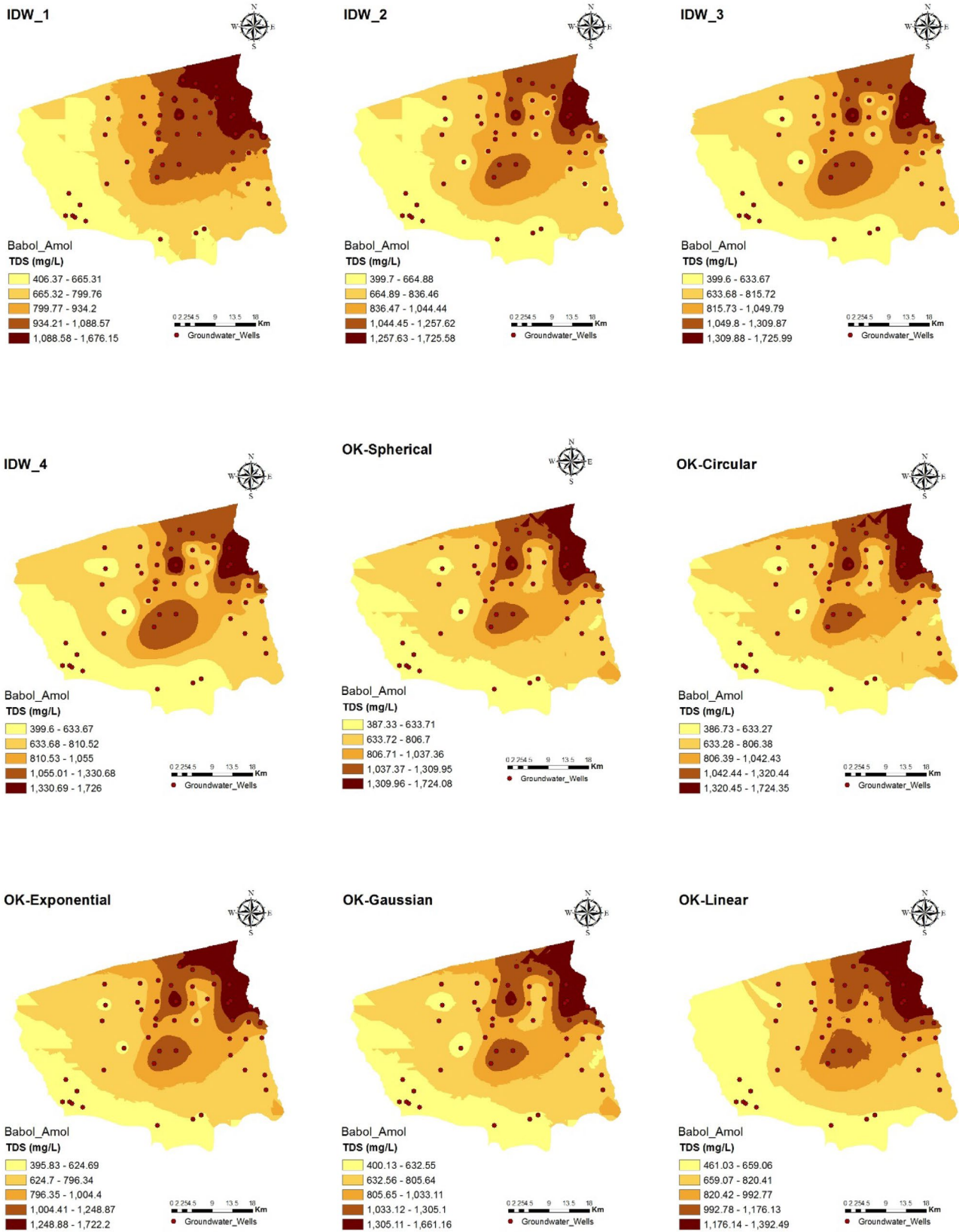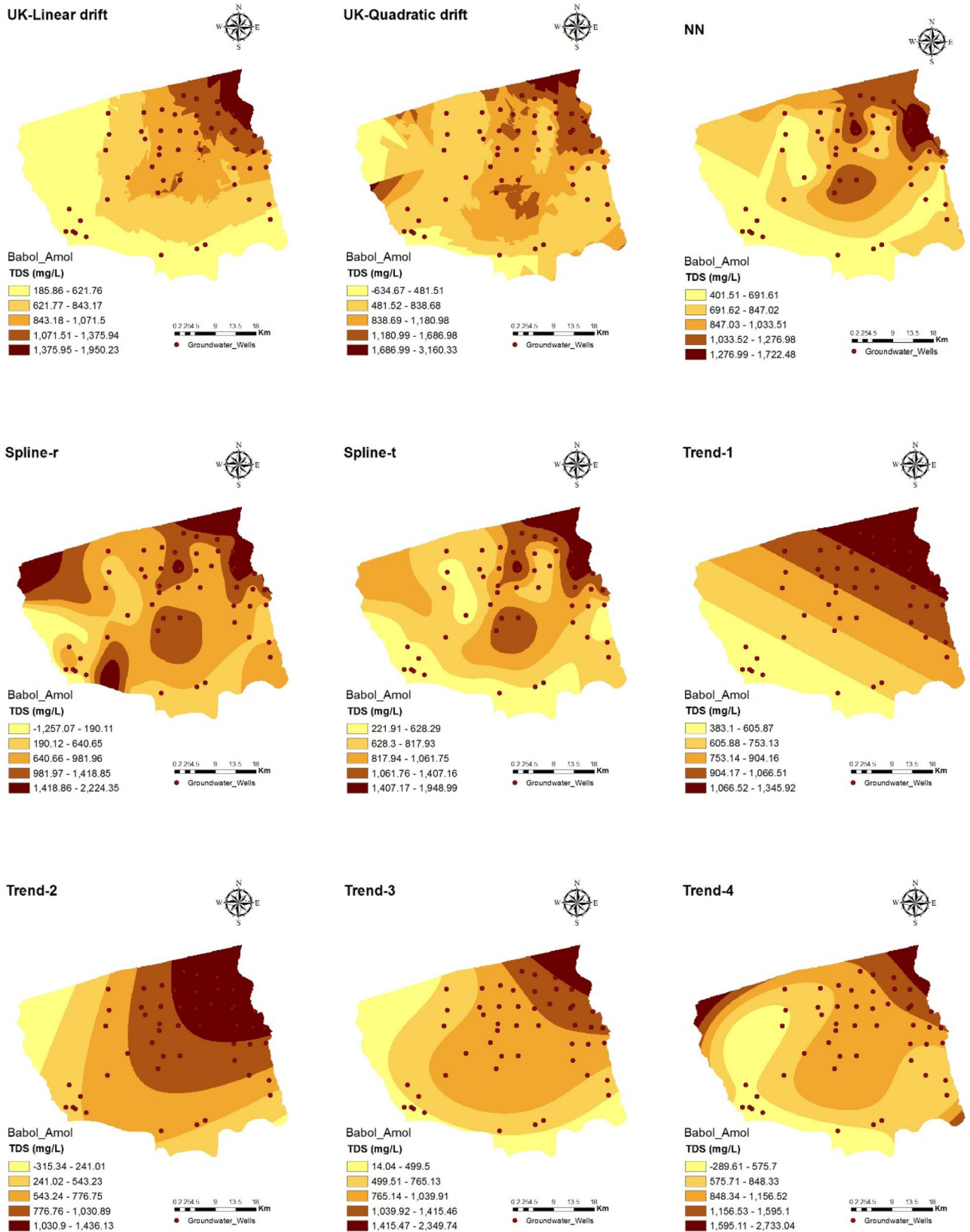
Fig. 7 (continued)

b

Fig. 7 (continued)

Fig. 7 (continued)

MRE, and MSE. Trend-1 yielded the most accurate result with the lowest values of ME. EBK-emp and EBK-logemp came in the next ranks, respectively. Log_OK and EBK-logemp, with NSE of almost 1, demonstrated the best results. The lowest |PBIAS| belonged to Trend-1. With the increase in the IDW power, there was a decrease in the values of MAE and MRE and an increase in NSE.

3. As a result, Log_OK method provided more accurate results with 57% of error criteria in Lenjanat and 71% in Babol–Amol aquifers. However, IDW method has also a good performance.

4. Furthermore, we can conclude that the interpolation pattern of the TDS concentration in shallow aquifers was not highly affected by different hydrogeological characterization. It could be due to some common points of view in these two shallow aquifers such as: existence of a Salt River in the Lenjanat plain vs. the Babol–Amol Coastal plain, shallow groundwater depth, almost the same groundwater transmissivity, agricultural activities, and a closed fresh river–aquifer interaction.

Table 2 Cross-validation performance and different interpolation methods ranking

Method	Area	RMSE	|ME|	MAE	MRE	MSE	NSE	|PBIAS|
IDW_1	Lenjanat	0.762	0.625	0.765	0.456	0.581	0.330	0.625
	Babol–Amol	0.583	0.509	0.697	0.531	0.339	0.197	0.509
IDW_2	Lenjanat	0.724	0.590	0.669	0.397	0.524	0.396	0.590
	Babol–Amol	0.544	0.494	0.625	0.465	0.296	0.300	0.494
IDW_3	Lenjanat	0.679	0.536	0.579	0.336	0.461	0.469	0.536
	Babol–Amol	0.534	0.511	0.587	0.435	0.285	0.326	0.511
IDW_4	Lenjanat	0.651	0.501	0.566	0.301	0.423	0.512	0.501
	Babol–Amol	0.542	0.541	0.577	0.429	0.294	0.305	0.541
OK-spherical	Lenjanat	0.757	0.595	0.799	0.479	0.574	0.339	0.595
	Babol–Amol	0.542	0.428	0.600	0.454	0.293	0.306	0.428
OK-circular	Lenjanat	0.757	0.595	0.799	0.479	0.574	0.339	0.595
	Babol–Amol	0.543	0.426	0.600	0.452	0.295	0.302	0.426
OK-exponential	Lenjanat	0.757	0.595	0.799	0.479	0.574	0.339	0.595
	Babol–Amol	0.531	0.427	0.591	0.448	0.282	0.332	0.427
OK-Gaussian	Lenjanat	0.757	0.595	0.799	0.479	0.574	0.339	0.595
	Babol–Amol	0.613	0.454	0.687	0.514	0.376	0.111	0.454
OK-linear	Lenjanat	0.757	0.595	0.799	0.479	0.574	0.339	0.595
	Babol–Amol	0.548	0.428	0.601	0.452	0.301	0.289	0.428
UK-linear drift	Lenjanat	0.720	0.795	0.724	0.395	0.518	0.403	0.795
	Babol–Amol	0.682	0.418	0.737	0.540	0.465	-0.101	0.418
UK-quadratic drift	Lenjanat	1.000	1.000	1.000	0.589	1.000	-0.153	1.000
	Babol–Amol	0.631	0.452	0.682	0.541	0.399	0.057	0.452
NN	Lenjanat	0.637	0.207	0.582	0.491	0.406	0.532	0.207
	Babol–Amol	0.521	0.540	0.590	0.465	0.271	0.358	0.540
Spline-r	Lenjanat	0.865	0.737	0.798	1.000	0.749	0.137	0.737
	Babol–Amol	1.000	1.000	1.000	1.000	1.000	-1.366	1.000
Spline-t	Lenjanat	0.737	0.124	0.685	0.595	0.543	0.374	0.124
	Babol–Amol	0.589	0.603	0.638	0.547	0.347	0.178	0.603
Method	Area	RMSE	|ME|	MAE	MRE	MSE	NSE	|PBIAS|
Trend-1	Lenjanat	0.772	0.552	0.815	0.511	0.595	0.314	0.552
	Babol–Amol	0.674	0.260	0.728	0.512	0.455	-0.075	0.260
Trend-2	Lenjanat	0.806	0.590	0.831	0.503	0.650	0.251	0.590
	Babol–Amol	0.731	0.533	0.855	0.635	0.534	-0.263	0.533
Trend-3	Lenjanat	0.799	0.569	0.817	0.469	0.638	0.264	0.569
	Babol–Amol	0.707	0.550	0.823	0.643	0.500	-0.184	0.550
Trend-4	Lenjanat	0.841	0.725	0.905	0.585	0.707	0.185	0.725
	Babol–Amol	0.620	0.503	0.675	0.524	0.384	0.091	0.503
EBK	Lenjanat	0.830	0.599	0.864	0.523	0.690	0.205	0.599
	Babol–Amol	0.529	0.492	0.583	0.450	0.280	0.337	0.492
EBK-emp	Lenjanat	0.827	0.594	0.806	0.497	0.685	0.211	0.594
	Babol–Amol	0.500	0.394	0.536	0.408	0.250	0.409	0.394
EBK-logemp	Lenjanat	0.727	0.384	0.715	0.493	0.529	0.391	0.384
	Babol–Amol	0.497	0.399	0.526	0.402	0.247	0.415	0.399
DK	Lenjanat	0.797	0.297	0.855	0.612	0.635	0.269	0.297
	Babol–Amol	0.497	0.482	0.577	0.449	0.247	0.415	0.482
log_OK	Lenjanat	0.572	0.153	0.479	0.305	0.327	0.623	0.153
	Babol–Amol	0.494	0.450	0.511	0.398	0.244	0.422	0.450
SK	Lenjanat	0.725	0.126	0.766	0.581	0.525	0.395	0.126
	Babol–Amol	0.510	0.505	0.583	0.460	0.260	0.385	0.505

Declarations

Conflict of interest The authors declare that they have no known competing financial interests or personal relationships that could have appeared to influence the work reported in this paper.

References

Afzal P, Madani N, Shahbeik S, Yasrebi AB (2015) Multi-Gaussian kriging: a practice to enhance delineation of mineralized zones by concentration volume fractal model in Dardevey iron ore deposit, SE Iran. J Geochem Explor 158:10–21. https://doi.org/10.1016/j.gexplo.2015.06.011

Aguilera AM, Aguilera-Morillo MC (2013) Comparative study of different B-spline approaches for functional data. Math Comput Model 58:1568–1579. https://doi.org/10.1016/j.mcm.2013.04.007

Arslan H (2012) Spatial and temporal mapping of groundwater salinity using ordinary kriging and indicator kriging: the case of Bafra Plain, Turkey. Agric Water Environ Manag 113:57–63. https://doi.org/10.1016/j.agwat.2012.06.015

Arslan H, Turan NA (2015) Estimation of spatial distribution of heavy metals in groundwater using interpolation methods and multivariate statistical techniques; its suitability for drinking and irrigation purposes in the Middle Black Sea Region of Turkey. Environ Monit Assess 187:516. https://doi.org/10.1007/s10661-015-4725-x

Babu BS (2016) Comparative study on the spatial interpolation techniques in GIS. Int J Sci Eng Res 7(2):550–554 **(ISSN 2229–5518)**

Barca E, Passarella G (2007) Spatial evaluation of the risk of groundwater quality degradation. A comparison between disjunctive kriging and geostatistical simulation. Environ Monit Assess 137:261–273. https://doi.org/10.1007/s10661-007-9758-3

Boufassa A, Armstrong M (1989) Comparison between different kriging estimators. Math Geol 21(3):331–345. https://doi.org/10.1007/BF00893694

Bryan R (1988) Introducing geostatistics-estimating spatial data. Critical water issues and computer applications. ASCE pp 374–379

Chilès JP, Delfiner P (2012) Geostatistics: modeling spatial uncertainty. Wiley, New York

Chiu C, Lin P, Lu K (2009) GIS-based tests for quality control of meteorological data and spatial interpolation of climate data. Mt Res Dev 29(4):339–349. https://doi.org/10.1659/mrd.00030

Costa JF (2003) Reducing the impact of outliers in ore reserves estimation. Math Geol 35(3):323–345. https://doi.org/10.1023/A:1023822315523

Cressie NAC (1993) Statistics for spatial data. Revised edition. A Wiley-Interscience Publication, New York

Dick J, Gerard B (2006) Optimization of sample patterns for universal kriging of environmental variables. Geoderma 138:86–95. https://doi.org/10.1016/j.geoderma.2006.10.016

Dowd PA (1982) Lognormal kriging: the general case. Math Geol 14(5):474–500. https://doi.org/10.1007/BF01077535

Duffy DJ, Germani A (2013) C# for financial markets, chapter 13: interpolation methods in interest rate applications. The Wiley Finance Series**(978-0-470-03008-0)**

Emery X (2008) Uncertainty modeling and spatial prediction by multi-Gaussian kriging: accounting for an unknown mean value. Comput Geosci 34(11):1431–1442. https://doi.org/10.1016/j.cageo.2007.12.011

Gol C, Bulut S, Bolat F (2017) Comparison of different interpolation methods for spatial distribution of soil organic carbon and some soil properties in the Black Sea backward region of Turkey. J Afr Earth Sci 134:85–91. https://doi.org/10.1016/j.jafrearsci.2017.06.014

Gong G, Mattevada S, O'Bryant SE (2014) Comparison of the accuracy of kriging and IDW interpolations in estimating groundwater arsenic concentrations in Texas. Environ Res 130:59–69. https://doi.org/10.1016/j.envres.2013.12.005

Gotway CA, Ferguson RB, Hergert GW, Peterson TA (1996) Comparison of kriging and inverse-distance methods for mapping parameters. Soil Sci Soc Am J 60:1237–1247. https://doi.org/10.2136/sssaj1996.03615995006000040040x

Hartkamp AD, De Beurs K, Stein A, White JW (1999) Interpolation techniques for climate variables. NRG-GIS Series 99-01. CIMMYT, Mexico, DF. https://repository.cimmyt.org/xmlui/bitstream/handle/10883/988/67882.pdf

Hosseini E, Gallichand J, Caron J (1993) Comparison of several interpolators for smoothing hydraulic conductivity data in South West Iran. Am Soc Agric Eng 36(6):1687–1693. https://doi.org/10.13031/2013.28512

Hu K, Li B, Lu Y, Zhang F (2004) Comparison of various spatial interpolation methods for non-stationary regional soil mercury content. Environ Sci 25(3):132–137

Hua Z, Debai M, Cheng W (2009) Optimization of the spatial interpolation for groundwater depth in Shule River Basin. Environ Sci Inf Appl Technol 2:415–418

Isaaks EH, Serivastava RM (1989) An introduction to applied geostatistics. Oxford University Press

Joseph J, Sharif HO, Sunil T, Alamgir H (2013) Application of validation data for assessing spatial interpolation methods for 8-h ozone or other sparsely monitored constituents. Environ Pollut 178:411–418. https://doi.org/10.1016/j.envpol.2013.03.035

Journel AG, Huijbregts ChJ (1978) Mining geostatistics. Academic Press, London

Keblouti M, Ouerdachi L, Boutaghane H (2012) Spatial interpolation of annual precipitation in Annaba-Algeria-comparison and evaluation of methods. Energy Procedia 18:468–475. https://doi.org/10.1016/j.egypro.2012.05.058

Khattak A, Ahmed N, Hussein I, Qazi A, Alikhan S, Rehman A, Iqbal N (2014) Spatial distribution of salinity in shallow Groundwater used for crop irrigation. Pak J Bot 46(2):531–537

Kitanidis P (1993) Geostatisitcs, chapter 20 in handbook of hydrology. McGraw-Hill, New York, p 1424p

Kravchenko AK, Bullock DG (1999) A comparative study of interpolation methods for mapping soil properties. Agron J 91:393–400. https://doi.org/10.2134/agronj1999.00021962009100030007x

Krivoruchko K (2011) Spatial statistical data analysis for GIS users. Esri Press, Redlands

Laslett GM, McBratney AB, Pahl PJ, Hutchinson MF (1987) Comparison of several spatial prediction methods for soil pH. J Soil Sci 38:325–341. https://doi.org/10.1111/j.1365-2389.1987.tb02148.x

Lee JJ, Jang CS, Wang SW, Liu CW (2007) Evaluation of potential health risk of arsenic-affected groundwater using indicator kriging and dose response model. Sci Total Environ 384:151–162. https://doi.org/10.1016/j.scitotenv.2007.06.021

Liu CW, Jang CS, Liao CM (2004) Evaluation of arsenic contamination potential using indicator kriging in the Yun-Lin aquifer (Taiwan). Sci Total Environ 321:173–188. https://doi.org/10.1016/j.scitotenv.2003.09.002

Liu R, Chen Y, Sun C, Zhang P, Wang J, Yu W, Shen Z (2014) Uncertainty analysis of total phosphorus spatial-temporal variations in the Yangtze River Estuary using different interpolation methods. Mar Pollut Bull 86:68–75. https://doi.org/10.1016/j.marpolbul.2014.07.041

Mare'chal A (1984) Recovery estimation: a review of models and methods. Geostatistics for natural resources characterization. Reidel, Dordrecht, pp. 385–420. https://doi.org/10.1007/978-94-009-3699-7_23

Martinez-Cob A (1996) Multivariate geostatistical analysis of evapotranspiration and precipitation in mountainous terrain. J Hydrol 174:19–35. https://doi.org/10.1016/0022-1694(95)02755-6

Mastroianni G, Milovanovic G (2008) Interpolation processes, basic theory and applications, Springer monographs in mathematics(9783540683469)

Meul M, Van Meirvenne M (2003) Kriging soil texture under different types of nonstationarity. Geoderma 112:217–233. https://doi.org/10.1016/S0016-7061(02)00308-7

Mirzaei R, Sakizadeh M (2015) Comparison of interpolation methods for the estimation of groundwater contamination in Andimeshk-Shush Plain, Southwest of Iran. Environ Sci Pollut Res 23:2758–2769. https://doi.org/10.1007/s11356-015-5507-2

Moyeed RA, Papritz A (2002) An empirical comparison of kriging methods for nonlinear spatial point prediction. Math Geol 34(4):365–386. https://doi.org/10.1023/A:1015085810154

Naoum S, Tsanis IK (2004) Ranking spatial interpolation techniques using a GIS-based DSS. Glob Nest Int J 6(1):1–20. https://doi.org/10.30955/gnj.000224

Nas B, Berktay A (2010) Groundwater quality mapping in urban groundwater using GIS. Environ Monit Assess 160:215–227. https://doi.org/10.1007/s10661-008-0689-4

Njeban HS (2018) Comparison and evaluation of GIS-based spatial interpolation methods for estimation groundwater level in AL-Salman District-Southwest Iraq. J Geogr Inf Syst 10:362–380. https://doi.org/10.4236/jgis.2018.104019

Plouffe CCF, Robertson C, Chandrapala L (2015) Comparing interpolation techniques for monthly rainfall mapping using multiple evaluation criteria and auxiliary data sources: a case study of Sri Lanka. Environ Model Softw 65:57–71. https://doi.org/10.1016/j.envsoft.2015.01.011

Puente CE, Bras RL (1986) Disjunctive kriging, universal kriging, or no kriging: small sample results with simulated fields. Math Geol 18(3):287–305. https://doi.org/10.1007/BF00898033

Pyrcz MJ, Deutsch CV (2014) Geostatistical reservoir modeling. Oxford University Press

Rhoades JD, Chanduvi F, Lesch S (1999) Soil salinity assessment: methods and interpretations of electrical conductivity measurements. FAO irrigation and drainage paper no. 57, Food and Agriculutre Organization of the United Nations: Rome, Italy. http://www.fao.org/3/x2002e/x2002e.pdf

Roth C (1998) Is lognormal kriging suitable for local estimation? Math Geol 30(8):999–1009. https://doi.org/10.1023/A:1021733609645

Rufo M, Antolín A, Paniagua JM, Jiménez A (2018) Optimization and comparison of three spatial interpolation methods for electromagnetic levels in the AM band within an urban area. Environ Res 162:219–225. https://doi.org/10.1016/j.envres.2018.01.014

Salekin S, Burgess JH, Morgenroth J, Mason EG, Meason DF (2018) A comparative study of three non-geostatistical methods for optimizing digital elevation model interpolation. Int J Geo-Inf 7(8):300. https://doi.org/10.3390/ijgi7080300

Schloeder CA, Zimmerman NE, Jacobs MJ (2001) Comparison of methods for interpolating soil properties using limited data. Soil Sci Soc Am J 65:470–479. https://doi.org/10.2136/sssaj2001.652470x

Shan Y, Tysklind M, Hao F, Quyang W, Chen S, Lin C (2013) Identification of sources of heavy metals in agricultural soils using multivariate analysis and GIS. J Soils Sediments 13(4):720–729. https://doi.org/10.1007/s11368-012-0637-3

Sterling DL (2003) A comparison of spatial interpolation techniques for determining shoaling rates of the Atlantic Ocean Channel. Master Thesis, Blacksburg, Virginia

Sun Y, Kang S, Li F, Zhang L (2009) Comparison of interpolation methods for depth to groundwater and its temporal and spatial variations in the Minqinoasis of northwest China. Environ Model Softw 24:1163–1170. https://doi.org/10.1016/j.envsoft.2009.03.009

Szypuła B (2016) Geomorphometric comparison of DEMs built by different interpolation methods. Landf Anal 32:45–58

Van Kuilenburg J, De Gruijter JJ, Marsman BA, Bouma J (1982) Accuracy of spatial interpolation between point data on soil moisture supply capacity, compared with estimates from mapping units. Geoderma 27:311–325. https://doi.org/10.1016/0016-7061(82)90020-9

Vicente-Serrano SM, Saz-Sanchez MA, Cuadrat MA (2003) Comparative analysis of interpolation methods in the middle Ebro Valley (Spain): application to annual precipitation and temperature. Clim Res 24:161–180. https://doi.org/10.3354/cr024161

Wang X, Ang Y, Cao Z, Zou W, Wang L, Yu G, Yu B, Zhang J (2013) Comparison study on linear interpolation and cubic B-spline interpolation proper orthogonal decomposition methods. Adv Mech Eng. https://doi.org/10.1155/2013/561875

Xie Y, Chen TB, Lei M, Yang J, Guo QJ, Song B, Zhou XY (2011) Spatial distribution of soil heavy metal pollution estimated by different interpolation methods: accuracy and uncertainty analysis. Chemosphere 82(3):468–476. https://doi.org/10.1016/j.chemosphere.2010.09.053

Yamamoto JK (2000) An alternative measure of the reliability of ordinary kriging. Math Geol 32(4):489–509. https://doi.org/10.1023/A:1007577916868

Yao L, Huo Z, Feng S, Mao M, Kang S, Chen J, Xu J, Steenhuis TS (2014) Evaluation of spatial interpolation methods for groundwater level in an arid inland oasis, northwest China. Environ Earth Sci 71:1911–1924. https://doi.org/10.1007/s12665-013-2595-5

Zimmerman D, Pavlik C, Ruggles A, Armstrong MP (1999) An experimental comparison of ordinary and universal kriging and inverse distance weighting. Math Geol 31(4):375–390. https://doi.org/10.1023/A:1007586507433